

Influence of temperature on tribological behavior of AlCoCrFeNi coatings prepared by electrospark deposition

H. L. Yang^a, X. M. Chen^a, L. Chen^b, Z. J. Wang^a, G. C. Hou^a, C. A. Guo^{a,*},
J. Zhang^a

^a*School of equipment Engineering, Shenyang Ligong University, Shenyang 110159, China*

^b*Chongqing Jianshe Industry (Group) LLC, Chongqing 400054, China*

AlCoCrFeNi high entropy alloy coatings were prepared on CrNi3MoVA steel by electrospark deposition technology, and their tribological behavior at different temperatures was investigated by utilizing a reciprocating friction and wear tester, and SEM, EDS and XRD were used to analyze the morphologies, composition and phase structure of AlCoCrFeNi coating. The results show that the as-deposited coating is composed of a single BCC structure with a hardness of 540 ± 40 HV_{0.1}. The wear resistance of AlCoCrFeNi coating at 600 °C is the best among 300 °C, 600 °C and 800 °C, and its wear rate is only 2.53×10^{-5} mm³/(N·m), which is one order of magnitude lower than that at the other two temperatures. At 600 °C, the main wear mechanism is oxidation wear, and a continuous compact oxide scale formed on the worn surface, which greatly improves the wear resistance of AlCoCrFeNi coating.

(Received May 12, 2022; Accepted January 27, 2023)

Keywords: High entropy alloy, AlCoCrFeNi coating, Electrospark deposition, Tribological properties

1. Introduction

High entropy alloy (HEA), a multi-component alloy material, has attracted wide attention for its unique properties and promising application prospect, thus it has become a hotspot in the field of alloy research. Since the HEA has no principal element, it usually consists of five or more alloying elements of equimolar, or atomic percentage of each element ranging from 5 to 35%. It is well known that HEAs combine the synergistic effect of high entropy, sluggish diffusion, severe lattice distortion and cocktail, and they can form simple solid solution structures, such as face centered cubic (FCC) and body centered cubic (BCC) structure rather than the complex intermetallic compounds. Recent studies have obtained many outstanding properties of HEAs, such as mechanical properties [1], high temperature oxidation resistance [2], corrosion resistance [3]. These desirable properties make HEAs have a great application potential in structural and functional materials.

* Corresponding author: bigocean1979@aliyun.com

HEAs can mainly be prepared by arc melting or casting, but it is difficult to manufacture due to the brittleness of most HEA bulks. However, HEA coatings prepared by surface coating technology (SCT) are cheaper and more practical than HEA bulks, thus the preparation of the HEA coatings on the surface of a low-cost alloy has attracted extensive attention from material scientists and engineers. Recently, researchers have tried to apply many modern surface technologies to prepare HEA coatings, such as magnetron sputtering (MS) [4], laser cladding (LC) [5], atmospheric plasma spraying (APS) [6], electrospark deposition (ESD) [7], gas tungsten arc (GTA) cladding [8], etc.

AlCoCrFeNi HEA possesses excellent properties of strength, hardness, wear resistance and corrosion resistance, therefore it has been one of the most widely investigated HEAs. Recently, AlCoCrFeNi coatings by different SCTs have shown promising application prospect in the field of aerospace, aviation, military, etc. Electrospark deposition (ESD), an effective green technology for preparing HEA coatings, has the advantages of low cost, excellent bonding strength and simple operation. Guo C A et al. [9] investigated the high-speed friction and wear performance of the ESD AlCoCrFeNi coating prepared on a CrNi3MoVA steel substrate, showing that the friction coefficient of the CrNi3MoVA steel is 0.85-0.95 while that of the AlCoCrFeNi coating only 0.29-0.38, and moreover the wear rate of the former is about 9.4 times that of the latter. In addition, their another investigation indicated that the ESD AlCoCrFeNi coating was about 41% reduction in wear rate compared with the electroplating hard Cr coating [10].

Although the ESD AlCoCrFeNi coating exhibits outstanding friction and wear performance in room temperature, to the best knowledge of the authors, there are still few relevant research reports on the friction and wear performance of ESD AlCoCrFeNi coatings on steel substrate at high temperature, and therefore the influence of temperature on the tribological behavior of the ESD AlCoCrFeNi coatings was investigated.

2. Material and methods

2.1. Preparation of the coating

The AlCoCrFeNi coating was deposited on the CrNi3MoVA steel sample with a size of 33 mm×14 mm×4 mm. The chemical composition of CrNi3MoVA steel is listed in Table 1. The Al, Co, Cr, Fe and Ni mixture powders with high purity were firstly melted in the high vacuum arc melting system. Then the cast AlCoCrFeNi HEA obtained by melting was cut into a cylindrical electrode with a size of $\Phi 5$ mm×36 mm and a cuboid for XRD analysis with a size of 15 mm×10 mm×2 mm by a wire cutting machine respectively.

Table 1. Chemical composition of CrNi3MoVA steel.

Element	Cr	Ni	Mo	V	Mn	C	Si	P	S	Fe
Wt.%	1.28	3.14	0.37	0.20	0.41	0.40	0.25	0.012	0.001	Balance

The AlCoCrFeNi coating was prepared by a DJ-2000 type adjustable power metal surface repair machine under the condition of argon protection. It was deposited in the center of the CrNi3MoVA steel sample surface with an area of 14 mm×14 mm. The deposition power was 1200 W, the electrode rotating speed was 2000 r·min⁻¹, the unit area deposition time was 2 min·cm⁻¹, and the flow rate of argon gas was 15 L·min⁻¹.

2.2. Characterization and testing of the coating

The surface morphology and composition of the AlCoCrFeNi coating were characterized by scanning electron microscope (SEM, Inspect F50, FEI Co., Hillsboro, Oregon) equipped with energy dispersive spectrometer (EDS, X-Max, Oxford instruments Co., Oxford, UK). The phase structure of the coating was obtained by X-ray diffraction (XRD, X 'Pert PRO, PANalytical Co., Almelo, Holland).

The hardness of the cross section of the coating was measured by Vickers hardness tester. The wear resistance of the coating was tested by MFT-5000 reciprocating friction and wear testing machine at 300 °C, 600 °C and 800 °C. The Si₃N₄ ceramic ball with a diameter of \square 9.25 mm was selected as the friction pair, the reciprocating distance was 6 mm, the frequency was 2 Hz, the load was 10 N, and the total friction time was 30 min. After the test, the samples were ultrasonically cleaned with acetone and alcohol mixture for 20 minutes.

3. Results and discussion

3.1. Microstructure and phase structure

Fig. 1. shows the surface morphology of the AlCoCrFeNi coating at different magnifications. As shown in Fig. 1a, it can be observed that there are traces of splats on the coating surface (marked by an arrow), which is the effect of high-speed plasma sputtering. As shown in Fig. 1b, it can be observed that the coating is composed of smooth and rough regions. EDS analysis is carried out on regions (A, B) and a dot (C) in the high-magnification image (Fig. 1b), and the results are shown in Table 2. In regions A and B, the content of Al, Co, Cr and Ni on the coating surface prepared by ESD are almost the same, but the content of Fe reaches 25-35 at.%, which is the result of the infiltration between electrode and substrate.

The EDS results also show that the content of Fe is higher in the smooth region B while it is slightly lower in the rough region A. Moreover, region A and B are very close to each other in position, but there is a large difference in Fe content, which may be caused by the rapid cooling speed in the process of EDS for the molten metal has solidified before mixing sufficiently. In Fig. 1b, the point C displays a white droplet feature, which should be the result of molten sputtering of the metal. The EDS results show that the content of O is 1.8% in the point C, which is believed that the oxidization still took place even under the protection of argon, and the oxide is very likely to be Al₂O₃ in light of thermodynamics calculation.

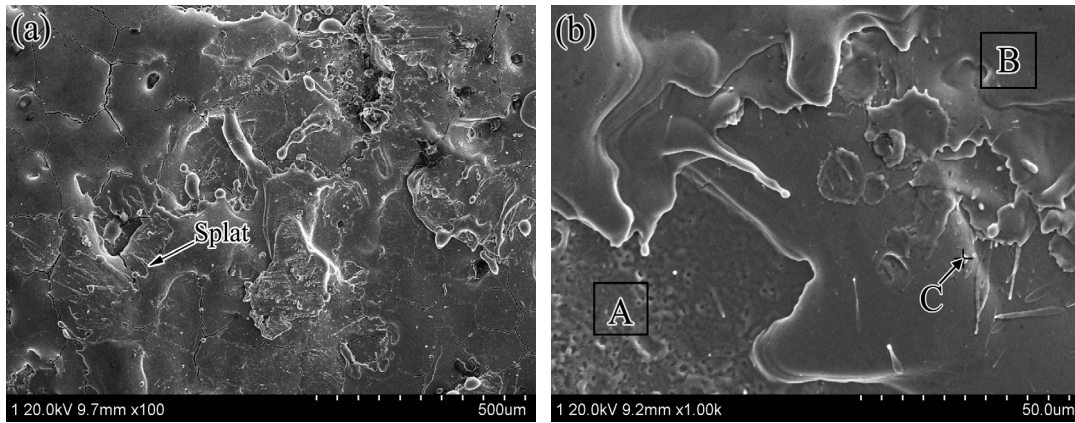


Fig. 1. Surface morphologies of AlCoCrFeNi coating at different magnifications.

Table 2. EDS results of two regions and a dot of AlCoCrFeNi coating.

Elements	Al (at.%)	Co (at.%)	Cr (at.%)	Fe (at.%)	Ni (at.%)	O (at.%)
region A	19.2	17.4	18.6	26.1	18.7	-
region B	17.4	16.1	17.9	32.0	16.6	-
Dot C	15.9	16.1	16.8	32.0	17.4	1.8

The XRD patterns of the as-cast AlCoCrFeNi and its ESD coating are displayed in Fig. 2. As shown in Fig. 1, the BCC and FCC are clearly identified in the XRD pattern of the as-cast AlCoCrFeNi. Comparatively, the ESD AlCoCrFeNi coating is composed of only BCC and B2 phase.

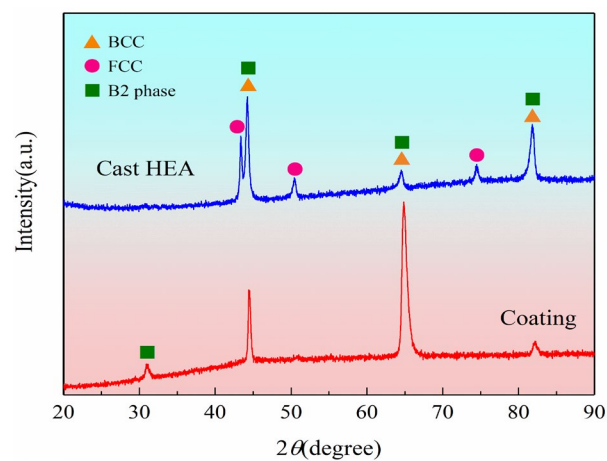


Fig. 2. XRD patterns of as-cast AlCoCrFeNi and its ESD coating.

According to reference [11], the content change of Al and Fe in AlCoCrFeNi HEA affects the phase structure. On one hand, Al is the most active among the five elements, which is prone to lose during the ESD process and then causes content change. In the

Al_xCoCrFeNi system, a single FCC requires less than 11 at.% Al content while a single BCC requires at least 18 at.% Al content. On the other hand, the AlCoCrFeNi coating is prepared on Fe-based alloy, and the infiltration between electrode and substrate will lead to higher Fe content in the AlCoCrFeNi coating in contrast to the cast AlCoCrFeNi electrode. The content of Fe in the AlCoCrFe_xNi alloy for less than 45 at.% generally has a single BCC structure; it is more than 47 at.%, BCC+FCC dual phase structure forms. Although the content of Al is less than 18 at.%, a single BCC still forms instead of BCC+FCC dual phase, indicating that the ESD process can be beneficial to the formation of a homogenous coating. Xie Y J et al. [12] used a NiCoCrAlYTa electrode with a dual phase γ/β structure to obtain a single γ coating by means of electrospark deposition.

3.2. Microhardness

The microhardness distribution along the depth direction in the cross-section of AlCoCrFeNi coating is shown in Fig. 3, and it can be roughly divided into three regions. The first region is the coating, and the microhardness is 540 ± 40 HV_{0.1}. The second region is near the interface between the coating and the substrate, and its mean microhardness is lower than that of the coating, but higher than that of the substrate. Furthermore, the microhardness of this region decreases with the increase of the depth. The third region is the substrate region, which maintains a microhardness of 390 ± 10 HV_{0.1}. The microhardness distribution tendency of the coating is similar to Chandrakant's results [13].

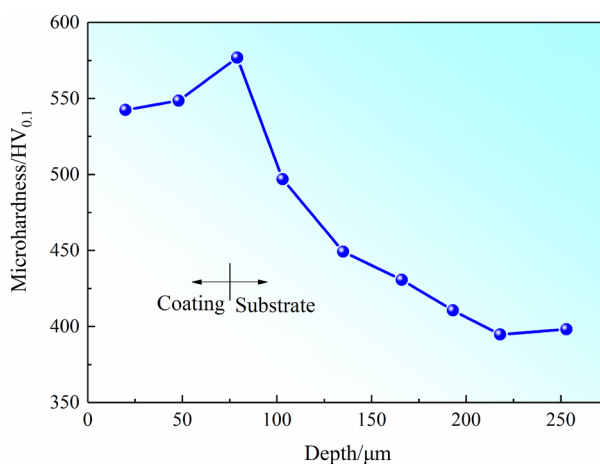


Fig. 3. Microhardness distribution along the depth direction in the cross-section of AlCoCrFeNi coating.

The microhardness of the coating is about 1.5 times that of the CrNi3MoVA steel substrate, which indicates that the AlCoCrFeNi coating may have better tribological properties than the CrNi3MoVA steel. As shown in Fig. 3, a very interesting phenomenon can be observed, which has never been reported about the ESD AlCoCrFeNi coating, i.e., in the substrate region close to the interface, about 10 μm along the depth direction, the microhardness of this region even exceeds that of the coating, which may be the result of solid-solution strengthening effect on the substrate by the elements from the AlCoCrFeNi electrode. This results still need further investigation to verify.

3.3. Wear behavior

The friction coefficient and wear rate of the AlCoCrFeNi coating at 300 °C, 600 °C and 800 °C are shown in Fig. 4. As shown in Fig. 4a, the friction coefficient of the coating fluctuates between 0.35 and 0.5 at different temperatures. The friction coefficient of three temperatures fluctuates obviously before 10 minutes, which was caused by the worn concave and convex between the friction pair. After 10 minutes, the friction coefficient gradually stabilizes and enters the steady stage. The friction coefficient increases slightly at 300 °C and 800 °C, and finally stabilizes between 0.42 and 0.45, respectively. The friction coefficient at 600 °C increases significantly from 0.33 to 0.42 for 8-12 min, and gradually stabilizes between 0.46 and 0.49.

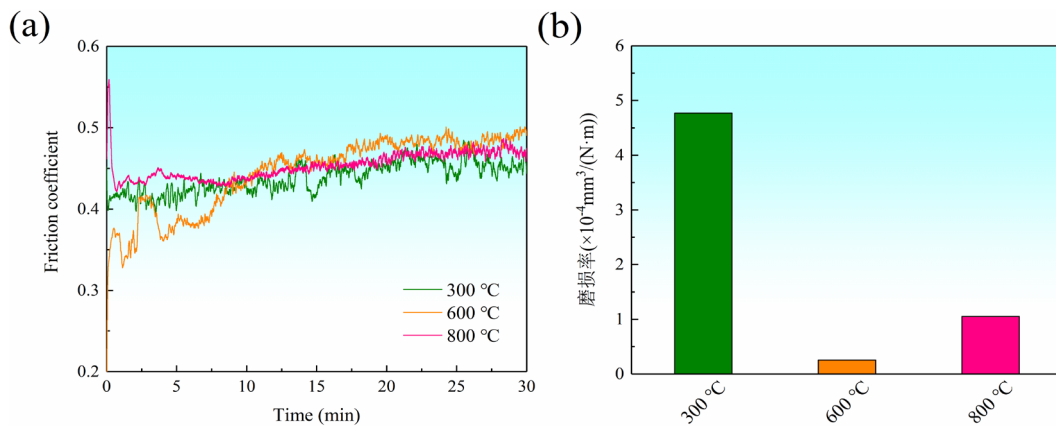


Fig. 4. Friction coefficient and wear rate of AlCoCrFeNi coating at 300 °C, 600 °C and 800 °C.

As shown in Fig. 4b, the wear rate of AlCoCrFeNi coating is $4.77 \times 10^{-4} \text{ mm}^3/(\text{N}\cdot\text{m})$, $2.53 \times 10^{-5} \text{ mm}^3/(\text{N}\cdot\text{m})$, $1.05 \times 10^{-4} \text{ mm}^3/(\text{N}\cdot\text{m})$ at 300 °C, 600 °C, 800 °C respectively. The wear rate of AlCoCrFeNi coating is the highest at 300 °C, about 19 times that at 600 °C and 4.5 times that at 800 °C. With the increase of temperature, the wear rate of AlCoCrFeNi coating will first decrease and then increase.

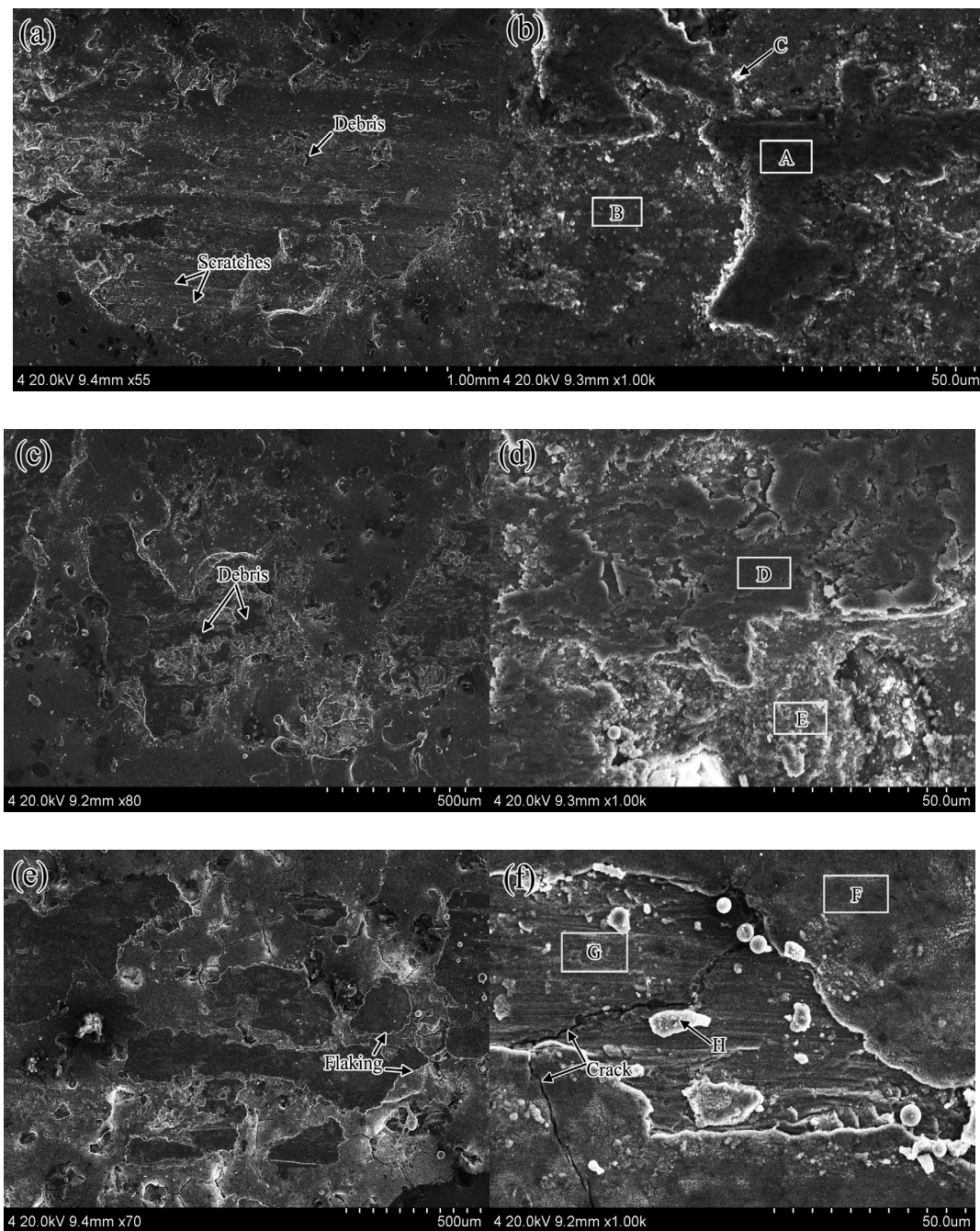


Fig. 5. SEM images of worn surfaces for the counter-body Si_3N_4 balls of the AlCoCrFeNi coating at 300 °C (a, b), 600 °C (c, d), 800 °C (e, f).

The SEM images of the worn surface of the AlCoCrFeNi coating at 300 °C (Fig. a, b), 600 °C (Fig. c, d) and 800 °C (Fig. e, f) are shown in Fig. 5, in which the low magnification images are on the left and the high magnification images on the right. The EDS results of the AlCoCrFeNi coating in the selected regions under high-magnification SEM images are shown in Table 3.

As shown in Fig. 5a, c, e, the grinding widths of the coating measured through the SEM images are 1.07 mm, 0.403 mm and 0.648 mm respectively. The three-dimensional morphologies of the worn surface of AlCoCrFeNi coating at 300 °C, 600 °C and 800 °C are shown in Fig. 6. The

roughness of the worn surface corresponding to 300 °C, 600 °C and 800 °C are 0.438 μm , 0.834 μm and 0.144 μm respectively.

As shown in Fig. 5a, there are plowing grooves like scratches appear on the worn surface at 300 °C (marked by arrows). Plowing grooves are generally the result of plastic shearing between the friction pair in the reciprocating movement. The particles produced by shearing will cause the fluctuations of the friction coefficient, which is consistent with the results in Fig. 4. Also, there is smooth wear debris (marked by an arrow) attached to the worn surface in Fig. 5a. The EDS analysis were carried out on the worn surface in Fig. 5b and the EDS results of region A, B, and C are listed in Table 3. The EDS results show that there is much O in region A, which means that the oxide is attached to the worn surface in region A. The content of O in region B is lower, so it can be inferred that region B does not undergo significant oxidation for it is still composed of five main elements of the coating. The Si and N from the grinding ball are mainly distributed in region A, indicating that the oxidized coating has better wear resistance compared with region B. In addition, the EDS results of the bright white powder (point C) in Fig. 5b show that it is Fe-rich oxide, which may be caused by Fe diffusing from the substrate through some defects. The wear debris generated by wear test adhere to the worn surface, and the flake-like oxide scale only covers part of the coating at 300 °C. The abrasive wear is the main wear mechanism, accompanying by oxidative wear at 300 °C.

As shown in Figure 5c, the worn surface is discontinuous, which may be caused by the large undulation of the coating surface and small worn quantity of the coating. There are no large plowing grooves on the worn surface, but more oxide debris is attached to the worn surface (marked by an arrow). The EDS analysis were carried out on the worn surface in Fig. 5d, and the EDS results of region D and E are listed in Table 3. The EDS results show that the obvious oxidation occurs in the region D with dark color and region E with light color, and the percentage of O in the two regions is 54.0% and 41.7% (at. %) respectively. The oxidation in the region D is more significant, so it is speculated that the oxide scale generated in region D is more compact and continuous. The appearance of a large number of oxide scale will be accompanied by adhesive wear, and the completeness of the oxidation region will cause a large roughness due to excellent wear resistance, which is proven by the roughness tests. Therefore, the friction coefficient of the coating is the highest among the three temperatures, as shown in Fig. 4. The worn surface of the coating is obviously oxidized at 600 °C, and the generated oxide scale completely covers the coating, avoiding the direct contact between the grinding ball and the coating. The oxidation wear is the main wear mechanism, accompanying by adhesive wear at 600 °C.

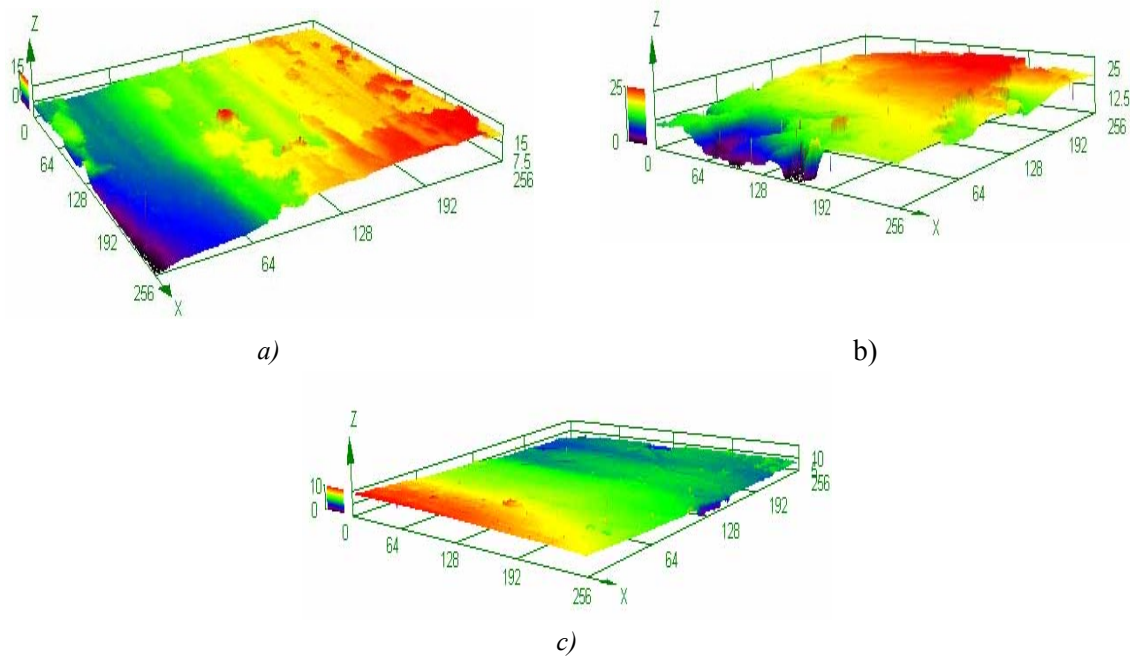


Fig. 6. Three-dimensional of worn surface: (a) 300 °C; (b) 600 °C; (c) 800 °C

As shown in Fig. 5e, there are traces of flakes on the worn surface (marked by arrows). Moreover, there are cracks (marked by an arrow in Fig. 5f) on the worn surface of the coating, which should be expanded cracks from the as-deposited coating due to thermal stress at high temperature. The EDS analysis was conducted on the morphology of worn surface in Fig. 5f. The worn surface is divided into two characteristic regions, one is region F with a smooth surface, and the other is region G with subtle plowing grooves. As shown in Table 3, the EDS results show that oxidation occurs in both regions F and G, and the percentage of O in the two regions is 53.0% and 21.6% (at. %) respectively, indicating that the oxide scale in region G had some spallation or re-produced after spallation. Moreover, the oxidation that occurred in the region F is more significant, and the oxide scale generated is more than that in the other two temperatures, which means that the oxidation became more severe with the improving temperature. The smooth worn surface can effectively decrease the friction coefficient due to the roughness reduction, which corresponds to the results in Fig. 4. In addition, the EDS point results of the white bulk H (marked by an arrow) in Fig. 5f show that the principal components are still Fe and O, indicating that more Fe diffusing from the substrate reacts with O with the increase of temperature. The main wear mechanism of the coating is still oxidation wear, accompanying by adhesive wear at 800 °C.

Table 3. EDS analysis results of selected regions in high magnification SEM image.

Regions		EDS quantitative results (at. %)							
		Al	Co	Cr	Fe	Ni	O	N	Si
300 °C	A	6.8	8.7	8.8	10.8	8.4	48.6	6.9	1.1
	B	15.0	16.3	21.2	21.2	21.7	4.5	0	0
	C	4.6	2.0	3.2	52.7	4.8	31.0	0	1.8
600 °C	D	7.4	5.4	7.8	9.0	6.5	54.0	3.4	6.4
	E	9.9	10.2	10.9	11.3	9.0	41.7	3.4	3.6
800 °C	F	6.5	11.6	8.6	12.6	6.5	53.0	0	1.3
	G	14.9	12.9	14.6	14.4	9.3	21.6	12.1	0.1
	H	6.3	1.7	3.8	38.3	2.4	47.5	0	0

Oxidation is a typical phenomenon during friction, and it will aggravate with the increase of temperature, which has a significant influence upon the tribological behavior of the friction pair. At 300 °C, the slight oxidation took place on the AlCoCrFeNi coating, and the oxide scale can not fully cover the surface of the coating (Fig. 5b, Table 2), thus the main wear mechanism is abrasive wear. At 600 °C, a continuous compact oxide scale formed on the coating and it greatly enhances the wear resistance of the coating (Fig. 5d, Table 2). According to the thermodynamic calculation, Al-rich or Cr-rich oxides will selectively form on the AlCoCrFeNi coating, and these oxides have outstanding hardness at high temperature. Furthermore, HEAs often have fine grain size even in cast state and the ESD process is beneficial for nanocrystalline forming in the coating due to its rapid solidification speed [9], and the oxide scale formed by the nanocrystalline coating always exhibits a strong adherence to the coating [14]. Both the above two reasons make the AlCoCrFeNi coating show excellent wear resistance at 600 °C. At 800 °C, the elevated temperature makes the oxidation aggravate further and the oxide scale becomes thicker, which will increase the stress in the oxide scale. When the stress is concentrated to a certain extent, the oxide scale will partly spall under the action of friction load (Fig. 5f, Table 2), which decreases the wear resistance of the coating.

Defects often appear within the ESD coating due to rapid solidification speed, especially for the coating with low plasticity. There are a few cracks in the ESD AlCoCrFeNi coating, which will become the fast diffusion tunnel for Fe (Fig. 5b, d, f). The Fe-rich oxide scale has poor adherence to the coating, which will decrease the wear resistance of AlCoCrFeNi coating. Therefore, it is important for AlCoCrFeNi coating with excellent wear resistance to control the defects through optimizing the parameters of ESD.

4. Conclusions

The dense ESD AlCoCrFeNi coating with only BCC structure can be prepared by using an AlCoCrFeNi electrode with dual BCC+FCC phase, and its microhardness is 540 ± 40 HV_{0.1}, about 1.5 times that of CrNi3MoVA steel. The steady friction coefficient of AlCoCrFeNi coating is 0.42-0.45 at 300 °C and 800 °C respectively and it is 0.46-0.49 at 600 °C.

The wear rate of AlCoCrFeNi coating is $4.77 \times 10^{-4} \text{ mm}^3/(\text{N} \cdot \text{m})$, $2.53 \times 10^{-5} \text{ mm}^3/(\text{N} \cdot \text{m})$ and $1.05 \times 10^{-4} \text{ mm}^3/(\text{N} \cdot \text{m})$ at 300 °C, 600 °C and 800 °C respectively, and it has the lowest wear rate at 600 °C. The main wear mechanism of AlCoCrFeNi coating is abrasive wear at 300 °C whilst it is oxidation wear at both 600 °C and 800 °C.

Acknowledgments

The authors are grateful for the financial support of the National Science Foundation of Liaoning Province of China (No.2019-ZD-0264), and the Research Project of application foundation of Liaoning Province of China (No.2022JH2/101300006), and the Supporting Project of Middle-young Aged Innovative Talents of Science and Technology of Shenyang City, and the Research Innovation Team Building Program of Shenyang Ligong University, and the Light-Selection Team Plan of Shenyang Ligong University.

References

- [1] Z. Lei, X. Liu, Y. Wu, H. Wang, S. Jiang, S. Wang, X. Hui, Y. Wu, B. Gault, P. Kontis, et al., *Nature* 563(7732), 546 (2018); <https://doi.org/10.1038/s41586-018-0685-y>
- [2] F. Zhang, L. Wang, S. Yan, G. Yu, J. Chen, F. Yin, *Materials Chemistry and Physics* 282(March), 125939 (2022); <https://doi.org/10.1016/j.matchemphys.2022.125939>
- [3] K. Kuwabara, H. Shiratori, T. Fujieda, K. Yamanaka, Y. Koizumi, A. Chiba, *Additive Manufacturing* 23 264 (2018); <https://doi.org/10.1016/j.addma.2018.06.006>
- [4] W. B. Liao, H. Zhang, Z. Y. Liu, P. F. Li, J. J. Huang, C. Y. Yu, Y. Lu, *Entropy* 21(2), 1 (2019); <https://doi.org/10.3390/e21020146>
- [5] G. J. Zhang, Q. W. Tian, K. X. Yin, S. Q. Niu, M. H. Wu, Y. N. Wang, J. C. Huang, *Jom* 73(11), 3597 (2021); <https://doi.org/10.1007/s11837-021-04874-w>
- [6] P. Shi, Y. Yu, N. Xiong, M. Liu, Z. Qiao, G. Yi, Q. Yao, G. Zhao, E. Xie, Q. Wang, *Tribology International* 151 106470 (2020); <https://doi.org/10.1016/j.triboint.2020.106470>
- [7] Q. H. Li, T. M. Yue, Z. N. Guo, X. Lin, *Metallurgical and Materials Transactions A: Physical Metallurgy and Materials Science* 44(4), 1767 (2013); <https://doi.org/10.1007/s11661-012-1535-4>
- [8] Q. Fan, C. Chen, C. Fan, Z. Liu, X. Cai, S. Lin, C. Yang, *Intermetallics* 138(92), 107337 (2021); <https://doi.org/10.1016/j.intermet.2021.107337>
- [9] C. Guo, Z. Zhao, S. Zhao, F. Lu, B. Zhao, J. Zhang, *Digest Journal of Nanomaterials and Biostructures* 13(4), 931 (2018).
- [10] C. Guo, Z. Zhao, S. Zhao, F. Lu, B. Zhao, J. Zhang, *Cailiao Daobao/Materials Reports* 33(5), 1462 (2019).
- [11] Q. Fan, C. Chen, C. Fan, Z. Liu, X. Cai, S. Lin, C. Yang, *Surface and Coatings Technology* 418(92), 127242 (2021); <https://doi.org/10.1016/j.surfcoat.2021.127242>
- [12] Y. J. Xie, M. C. Wang, *Journal of Alloys and Compounds* 480, 454 (2009); <https://doi.org/10.1016/j.jallcom.2009.01.100>
- [13] Chandrakant, N. S. Reddy, B. B. Panigrahi, *Materials Letters* 304, 130580 (2021);

<https://doi.org/10.1016/j.matlet.2021.130580>

[14] J. L. Wang, M. H. Chen, Y. X. Cheng, L. L. Yang, Z. B. Bao, L. Liu, S. L. Zhu, F. H. Wang, Corrosion Science 123, 27 (2017); <https://doi.org/10.1016/j.corsci.2017.04.004>